Impact of Star Polyacid Branching on Polymer Diffusion within Multilayer Films

Aliaksei Aliakseyeu¹, John F. Ankner², Svetlana A. Sukhishvili¹*

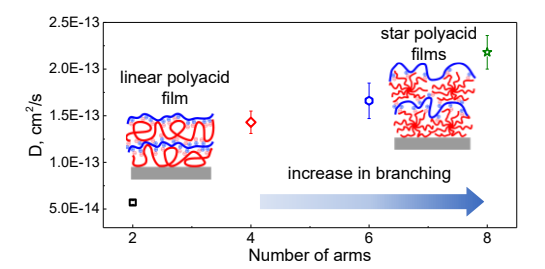
¹Department of Materials Science & Engineering, Texas A&M University,

College Station, Texas 77843, USA

² Spallation Neutron Source Second Target Station Project, Oak Ridge National Laboratory, Oak

Ridge, Tennessee 37831, USA

* (S.A.S.) Email: svetlana@tamu.edu



For Table of Contents use only

Abstract

A series of linear and star poly(acrylic acids) (LPAA and star PAAs) were synthesized to explore the effect of molecular architecture on the stratification and polymer dynamics of electrostatic layer-by-layer (LbL) films. Studies of LbL deposition of LPAA and star PAAs with poly[2-(dimethyl amino)ethyl methacrylate] (PDMAEMA) at acidic pH revealed an ~30 % increase in film dry thickness with increased polymer branching. Consistent with a greater mass of star polymer deposited within the films, in situ ellipsometric measurements of PAA uptake from solution revealed ~ 3.5-fold greater diffusion coefficients for 8-arm PAA in comparison to linear PAA. For comparison, the dynamics of the linear PDMAEMA partner was explored via neutron reflectometry (NR) studies of stacked multilayers containing hydrogenated and deuterated polycations, hPDMAEMA and dPDMAEMA. The stacked multilayers deposited from low-ionic-

strength solutions were stratified, exhibiting interfacial widths between hydrogenated and deuterated stacks of ~15 and 10 nm for films constructed with star and linear PAAs, respectively, suggesting relatively low mobility of the polycation in both assemblies. Further exposure of these films to 0.5 M sodium chloride solutions enhanced the mobility of PDMAEMA, revealing an order magnitude faster diffusion of PDMAEMA in films of 8-arm PAA relative to linear PAA. The faster diffusion of polymers within films of star polyacids was correlated not only with the compactness of star polymers, but also with an ~2-fold lower ionization of assembled 8-arm PAA as determined by Fourier transform infrared spectroscopy, and thus a lower number of polycation-polyacid ionic contacts in the case of star polymers as compared to their linear counterparts. The significant influence of molecular architecture on the number of polymer-polymer contacts was further confirmed by isothermal titration calorimetry studies of polyelectrolyte complexes in solution.

Introduction

Among polymers featuring a branched molecular architecture, star polymers are known for their simple structures consisting of only one branching point or core and polymer chains or arms attached to this core. The resulting compact molecular architecture differentiates the behavior of star polymers from that of their linear counterparts. For example, polymer branching results in a lowering of intrinsic viscosity, which is desirable in developing novel additives for lubricants. In addition, the prevalence of internal interactions and molecular rearrangements in star polymers compared to their linear counterparts contributes to enhanced energy dissipation of solvent-free thin films composed of star polymers during ballistic impact. Moreover, star polymer architecture is also advantageous for the development of novel drug and gene delivery systems.

¹⁰ In particular, star polymers have been demonstrated to have higher dye/drug trapping efficiency^{11, 12} and lower cytotoxicity^{13, 14} than linear polymers.

The advantages of star polymers as drug delivery containers have also been explored using layer-by-layer (LbL) films, such as those assembled using a star polycation (poly[2-(dimethyl amino)ethyl methacrylate], PDMAEMA) with insulin and glucose oxidase. Star PDMAEMA films released insulin upon exposure to glucose with no leakage into a control phosphate buffer saline solution. In contrast, films constructed with linear PDMAEMA continuously released insulin in the absence of glucose. ¹⁵ In another example, a temperature responsive 32-arm star polypeptide was assembled with tannic acid, and the resultant films showed sharp swelling transitions and temperature-triggered release of pyrene. ^{16, 17}

Despite these findings, the binding modes of star polymers within LbL films and the relationships between polymer topology, dynamics and internal film structure are not well understood. Previous reports on electrostatic assemblies of star polymers within LbL films yielded conflicting resuts, ¹⁸⁻²² with some studies suggesting slower ^{18, 19} and others faster diffusion ^{21, 22} of assembled star polymers relative to their linear counterparts, or no showing dependence on polymer branching at all. ²⁰ In one study, LbL assemblies of core-crosslinked crosslinked star PAA with linear poly(allylamine hydrochloride) (PAH) manifested higher polymer mass per deposition cycle in comparison with linear PAA/PAH systems ¹⁸ which was explained by the higher diffusivity of PAH within these films. Another study reported linear deposition of all-star PAA-PDMAEMA films which was explained by inhibited interdiffusion of high polymer molecular weight components. ¹⁹ Interestingly, assembly of these all-star films in acidic conditions formed highly porous films which were useful as high-surface-area substrates for enhanced protein binding. ²³ At the same time, in a different system composed of cyclodextrin-based star PDMAEMAs and

poly(styrene sulfonate) (PSS), a non-monotonous dependence was revealed between the degree of PDMAEMA branching and film growth and the observed differences in film growth were attributed to changes in the charge density of PDMAEMA.²⁰ An interesting observation was made by Choi *et.al.* who showed that star PDMAEMA/star PAA multilayer films can grow either similarly to or faster than linear PDMAEMA/PAA films depending on the pH of the assembly solutions.²¹ Contrary to other interpretations of binding between star and linear polymers, they suggested that star polymers can only bind through functional groups at the periphery of the molecules, leading to a large ionic pairing mismatch, lower effective ionic pairing and a possible increase in diffusivity of star polyelectrolytes.²¹

Note that prior studies made assumptions about star polymer diffusion based on the mode of film growth without the use of direct methods of measuring polymer dynamics such as neutron reflectometry (NR), fluorescence recovery after photobleaching bleaching or *in situ* ellipsometry. Here, to the best of our knowledge for the first time, we quantitatively explore the diffusion of star polyacids within LbL films using NR and *in situ* ellipsometry techniques. Additionally, we identify the relative contributions of two factors to the mobility of assembled polymers, namely the compactness of star polymers and the strength of their binding with linear polymer partners.

Materials and methods

Materials. Pentaerythritol (PTOL, synthesis grade) and dipentaerythritol (DPTOL, synthesis grade) used for synthesis of tetra and hexa-functional initiators were received from Merck. Tripentaerythritol (TPTOL, technical grade) used for synthesis of an octa-functional initiator was purchased from Sigma-Aldrich. Branched poly(ethylene imine) (BPEI), ethyl α-bromoisobutyrate (EtBiB) (98%), α-bromo isobutyril bromide (BIBB) (98%), tert-butyl acrylate, sodium hydroxide, isopropanol (ACS grade), dimethylformamide (DMF, ACS grade) copper (I)

bromide (99%), N,N,N',N",N"-pentamethyldiethylenetriamine (PMDETA), CDCl₃, and d₆-DMSO were purchased from Sigma-Aldrich. Aluminum oxide acidic (50-200 μM, 60 Å) and aluminum oxide basic (40-300 μM, 60 Å) of chromatography grade were obtained from Acros Organics. Hydrogenated poly[2-(dimethylamino)ethyl methacrylate] (*h*PDMAEMA, M_n 91 kDa, D=1.09) and deuterated poly[2-(dimethylamino)ethyl methacrylate] (*d*PDMAEMA, M_n 100 kDa, D=1.8) were purchased from Polymer Source. Chloroform (ACS grade), ethanol (ACS grade), hydrochloric acid (36.5%, ACS grade), sodium bicarbonate (ACS grade), and dichloromethane (ACS grade) were purchased from VWR. Trifluoroacetic acid (99%), and pyridine (99%) purchased from Alfa Aesar. All chemicals were used as received. Dialysis tubing (cutoff 3.5 kDa) was purchased from Thermo Scientific. Water used in this study was purified using a Millipore Milli-Q system.

Synthesis of pentaerythritol tetrakis(2-bromoisobutyrate) (4f-BiB), dipentaerythritol hexakis(2-bromoisobutyrate) (6f-BiB) and tripentaerythritol octakis(2-bromoisobutyrate) (8f-BiB). Synthesis of , 4f-BiB, 6f-BiB and 8f-BiB was performed as described elsewhere. ¹² 25 ml of dry dichloromethane, 10 ml (0.129 mol) of dry pyridine and 1 gram (0.029 mol of OH groups) of pentaerythritol were mixed in a flask containing a magnetic bar. The solution was cooled to 0 °C in an iced bath, and a solution of 7.3 ml (0.06 mol) of BIBB in 25 ml of dichloromethane was added dropwise through a syringe within 30 minutes under vigorous stirring. The reaction mixture was incubated for 24 hours at room temperature, and chloroform was added while the solution was stirred for additional 30 minutes. The resulting solution was triple washed with each of 10% HCl, 5% solution of NaHCO₃ and distilled water until pH of the distilled water remained neutral. The resulting solution was sequentially passed through basic and acidic SiO₂ columns and dried over sodium sulfate overnight. This was followed by a removal of

dichloromethane and chloroform by rotary evaporation and recrystallization of the residual liquid containing 4f-BiB in isopropanol. **Fig. S1** shows ¹H NMR spectra of 4f-BiB, 6f-BiB and 8f-BiB.

Synthesis of linear and star poly(tert-butyl acrylates). Linear and star poly(tert-butyl acrylates) (PTBA) were synthesized using atom transfer radical polymerization (ATRP) as described previously.²⁴ Initiators for linear, 4-, 6- and 8-arm polymers were EtBiB, 4f-BiB, 6f-BiB and 8f-BiB, respectively. The initiators, copper (I) bromide, PMDETA and tert-butyl acrylate were mixed in the molar ratio of 1:x:x:1000 where x is 1, 4, 6 and 8 for EtBiB, 4f-BiB, 6f-BiB and 8f-BiB (30 mg, 22 mg, 27 mg and 2500 mg for 8f-BIB, CuBr, PMDETA and tert-butyl acrylate, respectively, for synthesis of 8-arm PTBA) in a Schlenk flask containing 10 ml of acetone and freeze-thawed 3 times before starting the polymerization. The flask was then filled with argon and placed into an oil bath heated to 50 °C and stirred for 12 hours. Polymerization was then stopped by cooling the mixture in liquid nitrogen. The mixture was diluted with acetone and passed through the basic SiO₂ column to remove residual copper. The polymers were precipitated in 1:1 (by volume) water/ethanol mixture and dried under vacuum overnight at 25°C. All polymers were then dissolved in DMF and characterized using gel permeation chromatography (GPC) equipped with multi-angle laser light scattering (MALLS) and viscometry detectors which were pre-calibrated using a 30 kDa polystyrene standard. The specific refractive index increments, dn/dc, were determined for all polymers using a refractive index (RI) detector as described elsewhere.¹² The determined number-average (M_n), weight-average (M_w) molecular weights, dispersity (Đ) and degree of branching are shown in **Table 1**, while the GPC traces and the raw data on determination of branching degrees are presented in Fig. S2.

Table 1. The number-average, weight-average molecular weights and dispersity for linear and star poly(tert-butyl acrylates) (precursors of polyacrylic acids) determined by multiangle light scattering and viscometry detectors.

| Polymer | M _n , kDa | M _w , kDa | Đ | Branching per molecule |
|-----------------|----------------------|----------------------|------|------------------------|
| LPTBA | 90.7 | 106.3 | 1.16 | - |
| 4-arm star PTBA | 92.8 | 100.2 | <1.1 | 4±0.05 |
| 6-arm star PTBA | 102.3 | 107.5 | <1.1 | 6.1±0.1 |
| 8-arm star PTBA | 94.6 | 98.4 | <1.1 | 8.1±0.1 |

Synthesis of linear and star poly(acrylic acids) (PAAs). 0.5 g (0.004 mol of polymer units) of linear or star PTBA was dissolved in dichloromethane in a 20-ml glass vial and 1 ml (0.013 mol) of trifluoroacetic acid was added to the vial under vigorous stirring and stirred overnight. The precipitated polymers were filtered and dissolved in water. Aqueous solutions of polymers were placed in dialysis tubes (cut off Mw = 3.5 kDa) and dialyzed against 0.001M aqueous HCl which was replaced every 12 hours for a total of 2 days. The solutions were then freeze-dried to yield powders of linear and star PAAs, whose ¹H NMR analysis in d₆-DMSO confirmed complete disappearance of the tert-butyl groups (Fig. S3).

Multilayer build-up. Multilayers of linear and star PAAs and PDMAEMA were deposited on silicon substrates using the LbL dip deposition technique. The silicon wafers were cleaned as described elsewhere²⁵ and primed by adsorption of a BPEI monolayer by immersing in 0.2 mg/ml BPEI solution at pH 6 for 15 minutes. LbL films were then constructed via alternating adsorption of 0.2 mg/mL linear or star PAA and PDMAEMA from solution in 0.01 M phosphate buffer at pH 2.5, using two rinsing solutions between deposition of the polyacids and the polycation.

Atomic Force Microscopy (AFM). Morphology of the films containing linear and star PAAs was probed using a Bruker-Dimension Icon AFM instrument. The specimens were prepared as a monolayer of PAA, or as a 3.5-bilayer film (PAA/PDMAEMA) $_3$ /PAA deposited on a BPEI-primed silicon wafer at pH 2.5. Imaging was performed using a silicon cantilever with a normal stiffness of Kn = 7.4 N/m and a resonance frequency of ~150 kHz.

Neutron reflectometry (NR). For NR studies, LbL films were deposited on BPEI-primed Si substrates in the following sequence: (PAA/hPDMAEMA)x(PAA/dPDMAEMA)y at pH 2.5, where x and y represent the different number of layers of hydrogenated and deuterated (H and D) stacks, respectively. NR measurements were performed at the Spallation Neutron Source Liquids Reflectometer (SNS-LR) at the Oak Ridge National Laboratory (ORNL). The reflectivity data were collected using a sequence of 3.4-Å-wide continuous wavelength bands (selected from 2.63 Å < λ < 16.63 Å) and incident angles (ranging over 0.6° < θ < 2.34°). The momentum transfer, $Q = 4\pi \sin \theta/\lambda$, was varied over a range of 0.008 Å⁻¹ < Q < 0.20 Å⁻¹. Reflectivity curves were assembled by combining seven different independently normalized wavelength and angle data sets together, maintaining a constant footprint and relative instrumental resolution of $\delta Q/Q = 0.023$ by varying the incident-beam apertures.

Scattering densities within hydrogenated and deuterated stacks were averaged, with each block exhibiting its characteristic thickness, scattering density, and interlayer roughness. Those characteristic parameters were adjusted until the reflectivity curve was best fitted (minimize χ^2).

Ellipsometric measurements. Thickness of deposited films in dry state was characterized by a variable angle spectroscopic ellipsometer (M-2000 UV-visible-NIR (370-1000 nm) J. A. Woollam Co., Inc., Lincoln, NE, USA) at four angles of incidence: 45°, 55°, 65° and 75°. The adsorption of linear and star PAA on pre-deposited LbL films was measured in situ using liquid

cell equipped with a temperature controller on the same ellipsometer. All data was fitted using Cauchy model as described in our previous publication.²⁶

Determination of pK_as of linear and star PAAs. The pK_as of PAAs of different molecular architecture were determined by potentiometric titration using 0.576 mg/ml solutions of linear and star PAAs (8mM) and 1.6 mg/ml of NaOH (10 mM). The pH-meter Oakton pH5+ (ThermoFischer Scientific) was calibrated with buffer solutions prior to the measurements. During the measurements, a pH-electrode was immersed into a 10-ml solution of PAA under constant stirring and an NaOH solution was added (at 0.1, 0.2- or 0.5-ml volumes) using a 25-ml burette (Eisco Lab, class A, 0.1 ml \pm 0.05). The pK_as were determined as the pH at which 50% neutralization of linear or star polyacids occurred.

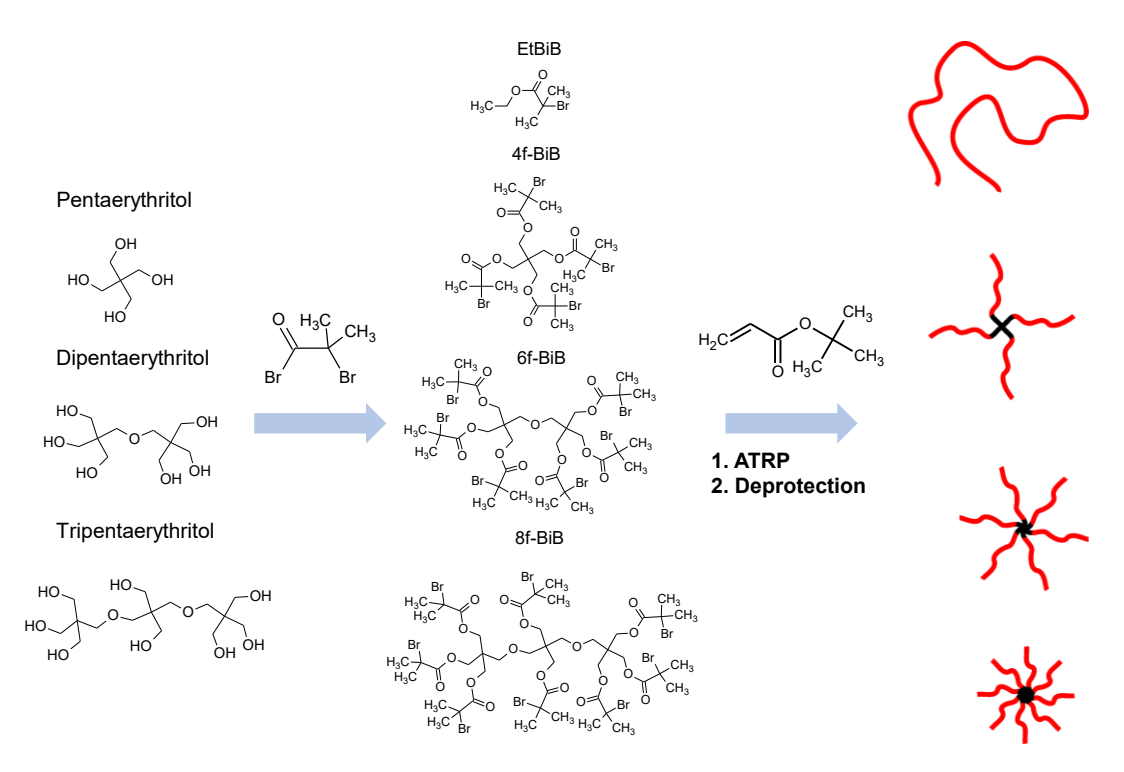
Fourier Transform Infrared (FTIR) Spectroscopy. 30-bilayer PDMAEMA/PAA LbL films were deposited onto undoped silicon wafers as described in the multilayer build-up section and were used in transmission FTIR measurements. All samples were analyzed with a Tensor II spectrophotometer (Bruker Optics GmbH, Germany). The FTIR band in the 1500-1800 cm⁻¹ region was deconvoluted to three Gaussian peaks centered at 1560 cm⁻¹ (asymmetric >COO⁻ stretching vibrations), 1710 cm⁻¹ (carbonyl vibration of non-ionized >COOH) and 1735 cm⁻¹ (ester group of the polycation) using the Origin Lab 2017 program. To quantify the ionization degree, the absorbance of the band corresponding to asymmetric >COO⁻ stretching vibrations at 1560 cm⁻¹ was compared with that of the carbonyl vibration of non-ionized >COOH group at 1710 cm⁻¹.

Isothermal titration calorimetry (ITC). 0.5 mg/ml solutions of linear and star PAA (7 mM unit concentration) and 0.63 mg/ml solutions of PDMAEMA (4 mM unit concentration) were first prepared in 0.01 M phosphate buffer and equilibrated overnight. Prior the experiments, pH in these solutions was adjusted to pH 2.5 using 1M HCl. ITC measurements were performed using

Nano-ITC instruments (TA Instruments, Inc.) at 25 °C at a stirring rate of 350 rpm. A 170-µl cell was filled with 0.5 mg/ml PAA solution and treated with thirty-three 1.5-µl injections of 0.63 mg/ml PDMAEMA at 180-second waiting intervals between injection. After completion of each titration, the cell was rinsed with 1 M NaOH to remove adsorbed hydrogen-bonded complexes from the cell walls, and repeatedly rinsed with deionized water and the 0.01 M phosphate buffer at pH 2.5. All titrations were repeated three times, and the results averaged. Fitting of the titration curves to obtain enthalpy, molar ratio, entropy and dissociation constant was performed using the NanoAnalyze Software.

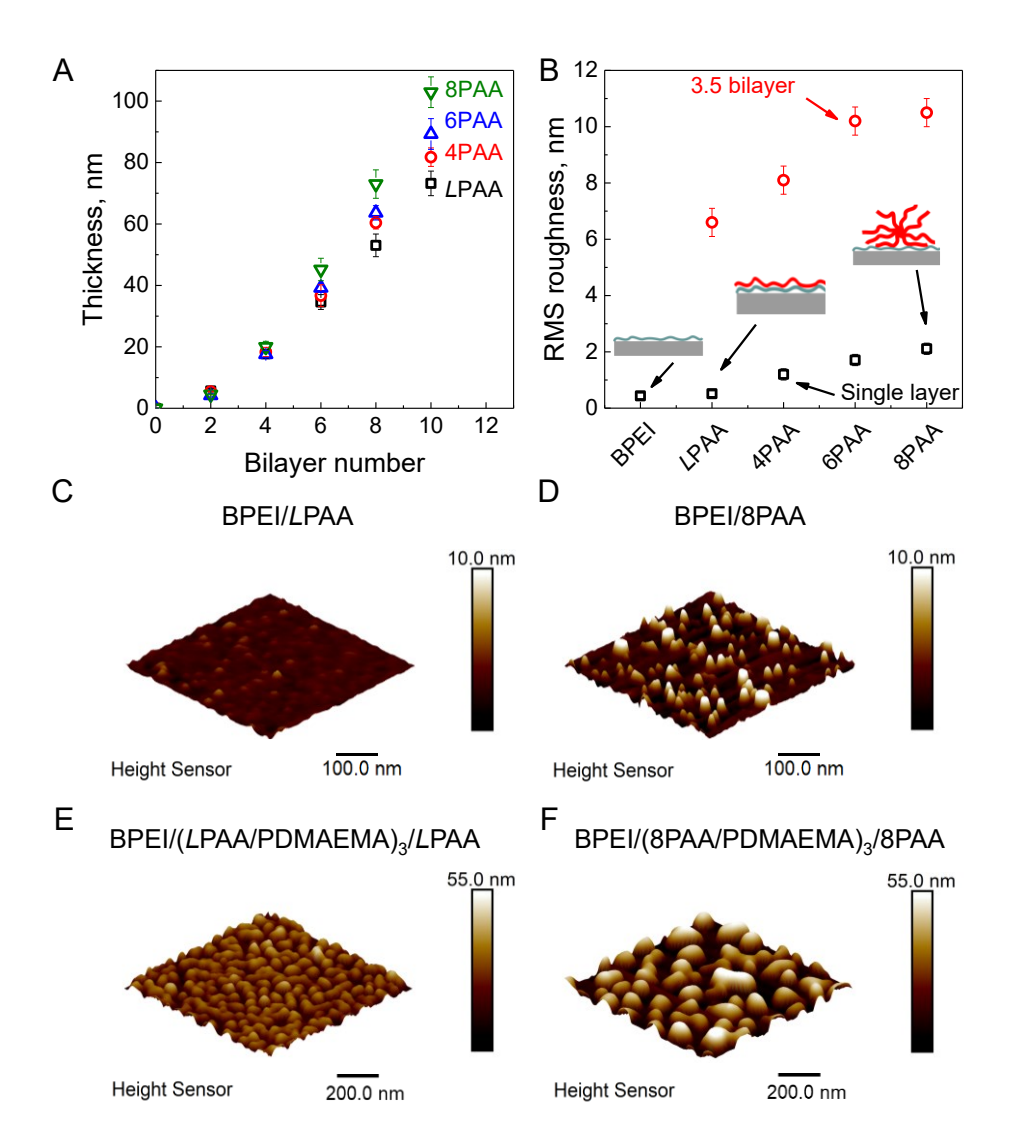
Results and discussion

To explore the effect of polymer branching on polymer dynamics within LbL films, we synthesized a series of polyacrylic acids (PAAs), *i.e.* linear and 4-, 6- and 8-arm star polymers, abbreviated as *L*PAA, 4PAA, 6PAA and 8PAA, respectively, using a core-first ATRP approach (Scheme 1). First, 4-, 6- and 8-arm ATRP initiators (4f-BiB, 6f-BiB and 8f-BiB) were synthesized through modification of pentaerythritol, dipentaerythritol and tirpentaerythritol with 2-bromoisobutyryl bromide. These initiators were used to perform polymerization using an established ATRP procedure²⁴ to yield linear, 4-, 6- and 8-arm poly(tert-butyl acrylates) (PTBA) polymers with matched molecular weights. The polymers were characterized using GPC equipped with MALLS and viscometry detectors that enable determination of absolute molecular weights and number of arms in star polymers (**Fig. S2**). This analysis confirmed that PTBAs with matched molecular weights of ~100 kDa and low dispersity (< 1.1 for star polymers) exhibited varied molecular architecture determined by the choice of ATRP initiator (**Table 1**). Deprotection of PTBA polymers using trifluoroacetic acid resulted in a family of star PAA polymers with different numbers of arms. ¹H NMR analysis shown in **Fig. S3** confirmed full deprotection of PTBA.



Scheme 1. Schematic path for synthesis of linear and star PAAs.

Fig. 1A shows ellipsometric thicknesses of dry multilayer films, illustrating construction of LbL assemblies using linear or star PAAs and PDMAEMA from solutions at pH 2.5. At such a low pH, individual linear and star PAAs are expected to be fully protonated (pK_a 6.45 and 6.7 for LPAA and 8PAA, respectively, as shown in Fig. S4) and form intramolecular hydrogen bonds.²⁷ However, the presence of a polycation can induce PAA ionization via ionic pairing, enabling electrostatic assembly of PAA in these conditions.²⁸ For LbL films, the degree of ionization is dependent on polycation charge density and the chemical nature of the cationic units.²⁹⁻³¹ As shown in Fig. 1A, all the films demonstrated non-linear growth up to 6th bilayer and linear growth at higher bilayer numbers – a phenomenon previously observed for several types of polyelectrolyte LbL films.³¹⁻³⁴ Note that higher-branched PAAs formed thicker layers, indicated by the ~30% greater thickness of 10-bilayer films of 8PAA/PDMAEMA compared to LPAA/PDMAEMA. Non-linear growth is often interpreted as a sign of weak binding within LbL



Ellipsometric thickness of dry LPAA/PDMAEMA 1. (A) (open squares), 4PAA/PDMAEMA (open circles), 6PAA/PDMAEMA (open triangles) 8PAA/PDMAEMA (open diamonds) films constructed from 0.2 mg/mL aqueous polymer solutions at pH 2.5. (B) RMS roughness of the BPEI-primed silicon substrate and single PAA layers or 3.5-bilayer PAA/PDMAEMA films with increasing PAA branching deposited on top of the priming layer, as well as the corresponding AFM images of (C) 500 nm × 500 nm dry $500 \text{ nm} \times 500 \text{ nm} \text{ BPEI/8PAA, (E)} 1$ BPEI/LPAA, (D) $\mu m \times 1 \mu m$ BPEI/(LPAA/PDMAEMA)₃/LPAA and (F) 1 μm × 1 μm BPEI/(8PAA/PDMAEMA)₃/8PAA films. AFM images for films constructed with 4PAA and 6PAA are shown in Fig. S5. The AFM experiments were performed with dry films exposed to ambient air with a relative humidity of 40%.

films,³⁵ and larger mass deposited per deposition cycle – indirect evidence of higher molecular diffusivity. Following this line of argument, one can infer faster interdiffusion of more highly branched PAAs.

Note that surface morphology can vary with the strength of polymer-polymer interactions, type of LbL building blocks and/or the growth mode of multilayer assemblies. 36-38 While linearlygrown electrostatic films tend to have smooth featureless morphologies, nonlinear films can exhibit grainy morphology.³⁶ At the same time, further exposure of electrostatic LbL films to salt solutions can trigger surface smothering that was attributed to enhanced polymer diffusivity. ^{39, 40} Fig. 1 B-F and Fig. S5 show AFM images of single layers of linear and star PAA assembled on top of BPEI-primed silicon wafers at pH 2.5. A gradual increase in surface roughness from 0.5 nm to 2 nm for LPAA and 8PAA adsorbed layers suggests that deposition of star polymers enhances surface roughness. Computational studies of the adsorption of polymers on solid surfaces have revealed the significant influence of polymer branching, solvent quality, and the strength of polymer-surface interactions on the conformation of adsorbed molecules. Specifically, flattening of star molecules has been predicted for low polymer branching and strong polymer-surface interactions, while preservation of particle-like morphology is expected for high polymer branching and weak polymer-surface interactions.⁴¹ Similarly, in this study LPAA can form a higher number of ionic contacts with the underlying BPEI layers and flatten during adsorption, leading to relatively smooth surfaces. By contrast, we suggest that star PAAs ionically pair with BPEI only via their peripheral units leading to a grainy morphology. For thicker 3.5-bilayer films, the trend of greater roughness for star-containing films persisted, though significant roughness also developed on LPAA/PDMAEMA films, probably due to the presence of a significant fraction of protonated hydrogen bonded polyacid units not participating in ionic pairing with the polycation.

Note that the increased roughness of star-PAA-containing films did not affect the overall quality of the film and the deposition could proceed at least to 30 bilayers *i.e.*, thicknesses exceeding 450 nm.

To quantitatively explore polymer interdiffusion in the films constructed using linear and star polymers, we employed neutron reflectometry (NR) – a non-invasive technique previously used to study the internal structure of LbL films and determine diffusion coefficients of linear polymers within multilayer assemblies. $^{26,\,42-44}$ We have used a previously described approach that involves decomposing the scattering length density (SLD or Σ) of the layer into molar fractions of PAA, hydrogenated PDMAEMA (hPDMAEMA), deuterated PDMAEMA (dPDMAEMA), and water to fit the data and taking into account the fact that the mass density of the film can vary. $^{45-47}$ The SLD (Σ) of a compound is calculated as follows:

$$\Sigma = \rho \frac{N_A \sum_j b_j}{M} \equiv \rho S \tag{1},$$

where ρ is the mass density (g/cm³), N_A is Avogadro's number, $\sum_j b_j$ is the sum of the scattering lengths of the nuclei in the polymer or water unit, M is the atomic mass of that unit, and S is a normalized scattering length density. In this way, we can separate the mass density from S for each of the components of the film (PAA, hPDMAEMA, dPDMAEMA and H_2O) and treat mass density as a fitted parameter for the film (ρ_f). Hence, the SLD of the H-stack ($\Sigma_{H\text{-stack}}$) is calculated as follows:

$$\Sigma_{\text{H-stack}} = \rho_f \times \left\{ w_{\text{H}_2\text{O}} S_{\text{H}_2\text{O}} + (1 - w_{\text{H}_2\text{O}}) \times \left[f_{\text{PDMAEMA}} \times \left(w_{d\text{PDMAEMA}} \frac{M_{d\text{PDMAEMA}}}{M_{h\text{PDMAEMA}}} S_{d\text{PDMAEMA}} + \{1 - w_{\text{H}_2\text{O}} + (1 - w_{\text{H}_2\text{O}}) \times \left[f_{\text{PDMAEMA}} \right] + (1 - f_{\text{PDMAEMA}}) S_{\text{PAA}} \right] \right\}$$

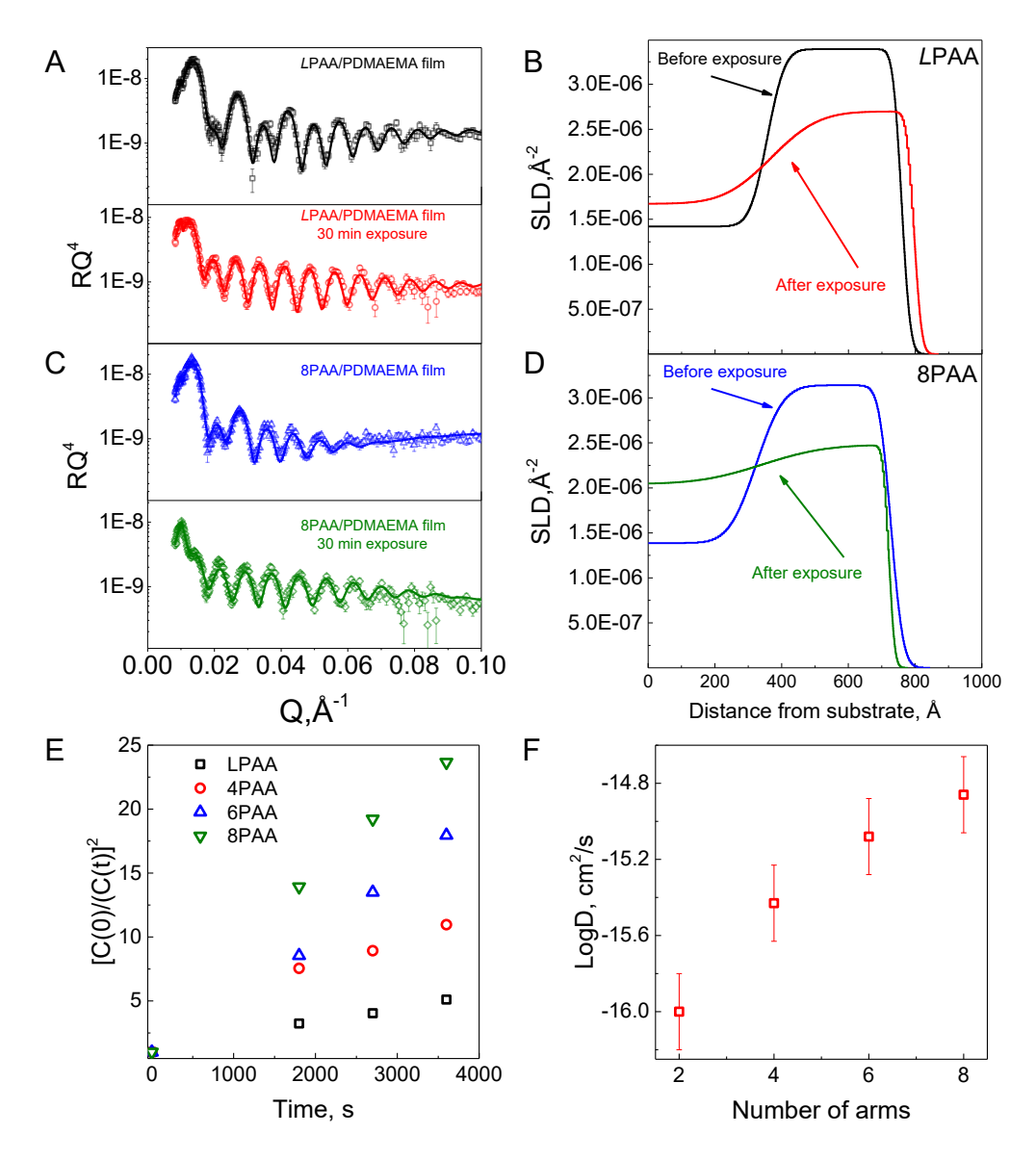


Fig. 2. Neutron reflectivity data (plotted as RQ^4 to enhance small features) and the corresponding fitted scattering length density profiles for (LPAA/hPDMAEMA)₅/LPAA/dPDMAEMA)₃ (A,C)and (8PAA/hPDMAEMA)₄/8PAA/dPDMAEMA)₃ (B,D) dry films before and after exposure to 0.5 M NaCl. (E) $[C(0)/C(t)]^2$ vs. time plot for LPAA/PDMAEMA (squares), 4PAA/PDMAEMA (circles), 6PAA/PDMAEMA (up triangles), 8PAA/PDMAEMA (down triangles) films. (F) Diffusion coefficients of PDMAEMA within LbL films containing linear and star PAA. The SLD profiles in Figs. 2B and 2D do not show the Si, SiO₂ and BPEI layers used in the fitting procedure. The full SLD profiles are shown in Fig. S10.

where w_{H_2O} is the molar fraction of water in the film, and S_{H_2O} , $S_{dPDMAEMA}$, $S_{hPDMAEMA}$, and S_{PAA} are normalized scattering length densities of water, dPDMAEMA, hPDMAEMA and linear or star PAA respectively (shown in Table S2) (Å⁻² g⁻¹ cm³). f_{PDMAEMA} is the molar fraction of PDMAEMA in the polymer portion (PAA/PDMAEMA) of the film which is consistent with the ellipsometry measurements of sequential film thicknesses during the deposition. $w_{dPDMAEMA}$ is the molar fraction of dPDMAEMA of the total PDMAEMA content of the H-stack, and M_{dPDMAEMA} and M_{hPDMAEMA} are molecular weights of the units of deuterated and hydrogenated PDMAEMAs, respectively. The $M_{dPDMAEMA}/M_{hPDMAEMA}$ ratio accounts for the increase in mass density with increasing fraction of deuterated material in the H-stack. The SLD of the D-stack ($\Sigma_{D\text{-stack}}$) was calculated in a similar manner (described in the Supporting Information). Fig. 2 and Figs. S6-9 show the specular neutron reflectivity of films as deposited and after exposure to 0.5 M NaCl solution at pH 2.5. Interestingly, the as-deposited films were well stratified for PAA of all molecular architectures (**Tables S2-3, S7, S11, S15**, internal roughnesses (σ_{int}) 9.8, 11.8, 14.0 and 15.2 nm for LPAA-, 4PAA-, 6PAA- and 8PAA-containing films, respectively), suggesting low mobility of PDMAEMA within the multilayers. Good stratification of films is also supported by the absence of deuterated PDMAEMA in the nominal H-stacks for all films (Tables S3, S7, S11, S15). Yet, a higher σ_{int} between H and D-stacks was observed for the film containing 8PAA (~15 nm) which was ~1.5 fold higher than for LPAA/PDMAEMA films (~10 nm) (**Table S2**). This effect can be related to less uniformity in films containing star polymers whose air/film roughness obtained from NR was higher than that for films of linear polymers (6.4 nm for 8PAA/PDMAEMA vs. 4.8 nm for LPAA/PDMAEMA films), in good agreement with the AFM data.

To induce PDMAEMA diffusivity, we then exposed the as-assembled films to a 0.5 M NaCl solution for 30, 45 and 60 min (**Fig. 2B, D, Figs. S6-S9**, and **Tables S4-S6, S8-S10, S12-S14, S16-S18**). Exposure to salt solution led to significant changes in all films, ranging from moderate mixing for linear PAA to nearly complete intermixing for the films containing 8PAA (**Fig. 2B, D**). Rapid diffusion of PDMAEMA under these conditions does not allow one to assume the existence of a semi-infinite reservoir (by tracking the linear dependence of the square root of σ_{int} with time). Instead, we have used a "limited source diffusion" model assuming Fickian diffusion of PDMAEMA in the direction vertical to the substrate^{48, 49} and quantifying the relative concentration of dPDMAEMA (C(t)/C(0)) in the D-Stack as ratio of w_{d PDMAEMA at time t to w_{d PDMAEMA at time 0:

$$\frac{C(t)}{C(0)} = \frac{\sigma_0}{(2Dt + \sigma_0^2)^{1/2}},\tag{3},$$

where C(t) and C(0) are the concentrations of deuterated material in the D-stack at time t after exposure, and time 0 (*i.e.*, in the as-assembled film), respectively, σ_0 is the initial root-mean-square interfacial width between H and D-stacks determined as $\sigma_{int}/2.35$, ⁴⁴ D is the diffusion coefficient of PDMAEMA within the film. The detailed determination of C(t)/C(0) is described in the **Supporting Information**. Simple mathematical transformation of equation (3) leads to a linear dependence of the inverted relative concentration of dPDMAEMA squared as a function of time:

$$\left(\frac{C(0)}{C(t)}\right)^2 = \frac{2D}{\sigma_0^2}t + 1.$$
(4),

Fig. 2E plots $[C(0)/C(t)]^2$ vs. time. For all films, the time dependence was linear, and its slope increased with branching degree. Fitting these slopes allowed us to estimate diffusion coefficients for PDMAEMA of 1.0×10^{-16} , 3.7×10^{-16} , 8.2×10^{-16} and 1.4×10^{-15} cm²/s for

LPAA/PDMAEMA, 4PAA/PDMAEMA, 6PAA/PDMAEMA and 8PAA/PDMAEMA films, respectively (Fig. S11). These values are at least an order magnitude higher than the diffusion coefficient of PSS within PSS/poly(dimethyldiallyll ammonium chloride) (PDADMAC) LbL films consistent with the known tendency of PSS to form strong ionic pairs with polycations. At the same time, the reported diffusion coefficients are at least an order magnitude lower than the diffusion coefficient of quaternized PDMAEMA (QPC) in PMAA/QPC films, whose larger diffusion coefficients can be related to weaker ionic pairing in this system due to steric effects of the alkyl substituents on the amino group of QPC.

While NR studies revealed differences in diffusion of a PDMAEMA partner assembled with PAA of different molecular architectures, those experiments were not sensitive to the molecular mobility of the polyacid. To determine mobility of PAA, we have performed *in situ* ellipsometry experiments in which we adsorbed linear and star polymers onto preassembled LbL films and monitored wet film thickness as a function of time (**Fig. 3A**). **Fig. 3B** shows normalization of the polymer uptake (q) using the following equation: $q=(H_t-H_0)/(H_{\infty}-H_0)$, where H_0 is initial thickness of the wet films, and H_t and H_{∞} the effective (at time t) and equilibrated thicknesses of the wet films, respectively. While for with star PAAs the saturation plateau was reached relatively quickly (within ~1.6 min for 90% saturation), LPAA required more time to saturate (~5.5 min for 90% saturation), suggesting lower mobility of linear polyacid chains within LbL films. Assuming that polymer diffusion within LbL is Fickian, $^{26.50-52}$ we can estimate the diffusion coefficients by plotting (qH)²/4 versus t (**Fig. 3C**) and fitting the initial linear region to the following equation:

$$Dt = \frac{(qH_t)^2}{4} \tag{5},$$

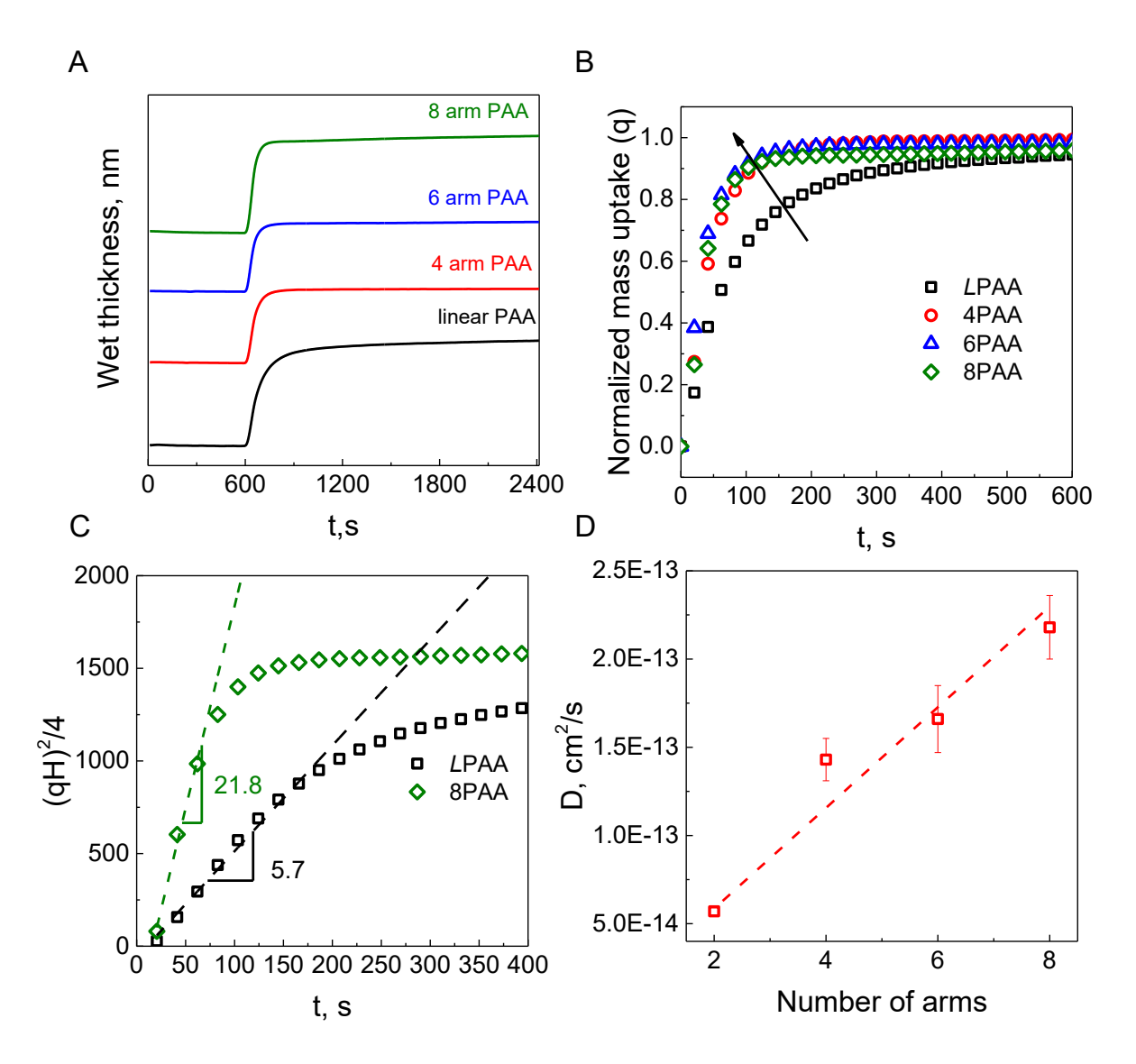


Fig. 3. (A) *In situ* ellipsometry thicknesses of PAA/PDMAEMA films when deposited PAA amounts were allowed to saturate. (B) Uptake kinetics of *L*PAA (squares), 4PAA (circles), 6PAA (triangles) and 8PAA (diamonds) by LbL films (40-45 nm dry thickness) containing PDMAEMA as the top layer. (C) $(qH)^2/4$ versus *t* dependence plotted for adsorption of *L*PAA (squares) and 8PAA (diamonds). The dashed lines represent fits to the linear region of polymer adsorption ($R^2>0.99$). (D) Diffusion coefficients versus number of PAA arms as calculated from the experiments on polyacid uptake kinetics by the swollen films.

Fig. 3D shows that the diffusion coefficients of PAA evaluated using this equation systematically increased with number of arms. This increase is consistent with a one-order-of-

magnitude decrease in the polycation-polyanion dissociation constant between LPAA and 8PAA. Two arguments can be suggested to rationalize faster diffusion of star polymers within LbL films. First, star polymers have a more compact structure and consequently a smaller hydrodynamic size. Consistent with this argument, diffusion of star polymers was experimentally found to be faster than that of linear polymers of equivalent molecular weight in experiments with individual polymers in solution.⁵³ Polymer chain compactness can be estimated using the contraction factor g defined as $g = \langle R_g^2 \rangle_s / \langle R_g^2 \rangle_l$, where $\langle R_g^2 \rangle_s$ and $\langle R_g^2 \rangle_l$ are the mean square radii of star and linear polymers of the same molecular weight.⁵⁴ In a good solvent, the contraction factor for a monodisperse polymer can be calculated via the following equation: g=(3f-2)/f² where f is the number of arms in a star.^{55, 56} This equation yields contraction factors 0.63, 0.44 and 0.34 for 4PAA, 6PAA and 8PAA, respectively. To further relate the radii of gyration and hydrodynamic radii, consider computational studies of star polymers with differing numbers of arms. These studies demonstrated that the R_h -to- R_g ratio increases with the number of arms from 0.9 for a linear to 1.15 for an 8-arm star polymer.⁵⁷ Hence, we can correlate the hydrodynamic radii of polymers of different molecular architecture with the radius of gyration of their linear counterpart of the same molecular weight as 0.9 $\langle R_g \rangle_l$, 0.77 $\langle R_g \rangle_l$, 0.71 $\langle R_g \rangle_l$ and 0.67 $\langle R_g \rangle_l$ for linear, 4-, 6- and 8arm polymers, respectively. Based on the scaling between diffusion coefficients and hydrodynamic radii $D \sim R_h^{-1}$, one can make a prediction that D should be ~1.35-fold higher for 8PAA in comparison to LPAA using these arguments. These estimates are consistent with light scattering studies of star polymer diffusion in solutions that reported an ~1.3-fold difference in diffusion coefficients for 3- and 12-arm polystyrene of matched molecular weight.⁵⁸ However, this predicted difference is much smaller than the 3.6-fold increase in D of 8PAA in comparison to LPAA observed in our experiments. Thus, compactness does not fully explain the higher diffusivity of star polymers within LbL films.

A second factor potentially contributing to the increase in star polymer mobility is the effect of PAA molecular topology on the strength of binding with the polycation. Because assembly of PAA within LbL films is stabilized by electrostatic pairing of ionized units of PAA with PDMAEMA, we should first consider the effect of molecular architecture on the ionization of individual PAA molecules in solution. Previous studies showed that the degree of ionization of weak polyelectrolytes in aqueous solution is strongly dependent on their molecular architecture, ¹⁸, ⁵⁹ reporting that star PAA had a higher pK_a compared to its linear counterparts due to higher osmotic pressure within the star polymers.⁵⁹ The potentiometric titration study performed herein confirmed that an increase in polymer branching resulted in a gradual increase of pK_a from 6.45 for LPAA to 6.75 for 8PAA (Fig. S4). While at the deposition pH 2.5, PAA of all molecular architectures is fully protonated prior to assembly with PDMAEMA, ionization can be induced after its inclusion within LbL films. We hypothesize that the differences in ionization of linear and star PAA correlate with the strength of binding of these polymers within LbL films and to the observed difference in polymer dynamics. Our aim was to correlate the ionization degree of assembled PAA (and thus the strength of PAA/PDMAEMA binding) with PAA dynamics. Specifically, we expected that the more highly ionized linear PAA formed more ionic pairs with PDMAEMA and slowed PAA mobility, while the fewer ionic contacts formed by less ionized compact star PAAs favors higher PAA mobility.

To test the above hypothesis, we explored ionization of linear and star PAAs within LbL assemblies using FTIR spectroscopy. The peaks associated with stretching vibrations of ionized

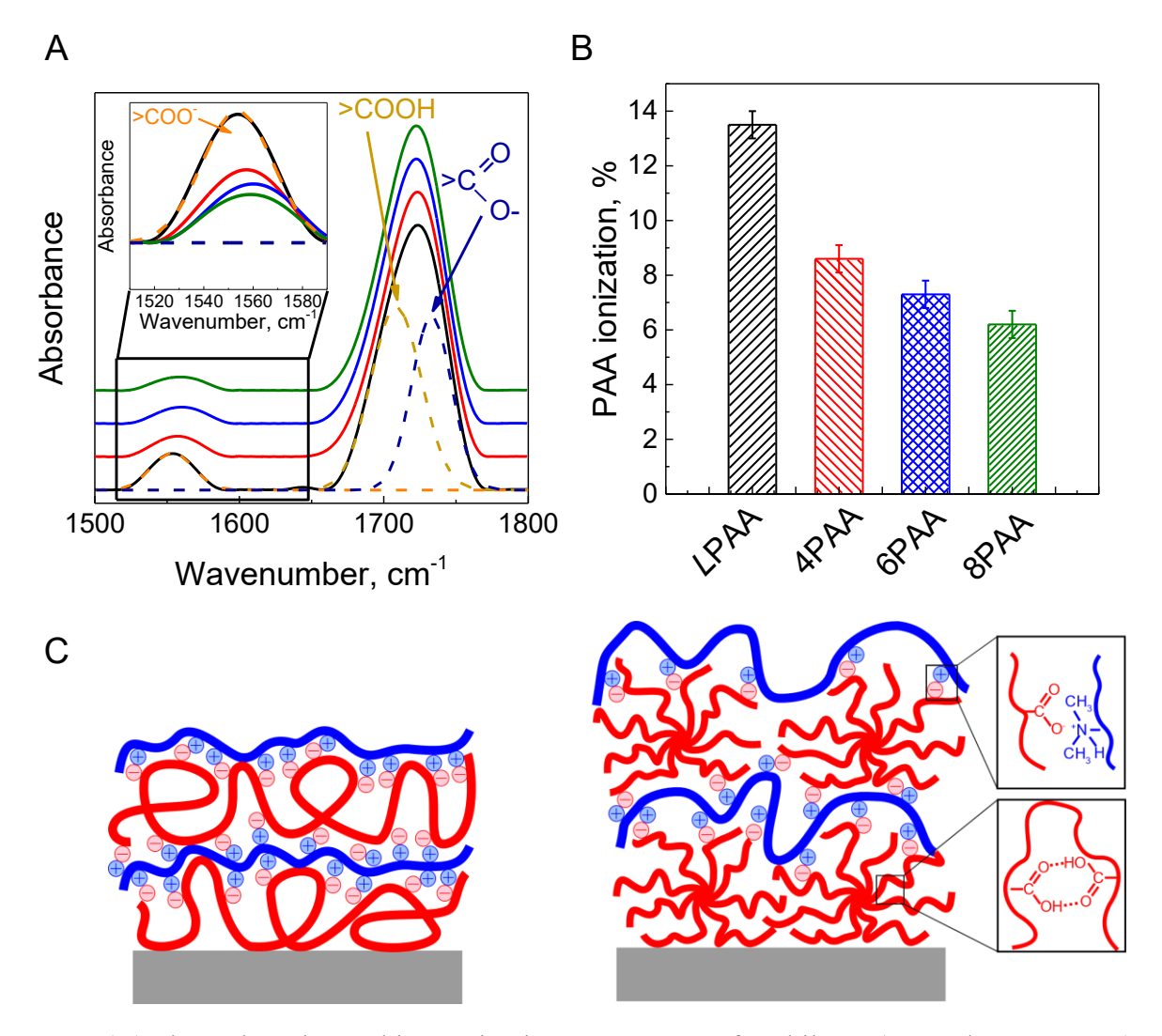


Fig. 4. (A) The carbonyl stretching region in FTIR spectra of 30-bilayer (LPAA/PDMAEMA)₃₀ (black), (4PAA/PDMAEMA)₃₀ (red), (6PAA/PDMAEMA)₃₀ (blue) and (8PAA/PDMAEMA)₃₀ (green) LbL films deposited at pH 2.5, also showing vibrational bands of the carboxylate ion (v_{COO^-}) of PAA and deconvolution of absorbances of carboxylic groups (v_{COOH}) of PAA and the ester group of PDMAEMA ($v_{C=O}$) for the LPAA/PDMAEMA film. Inset shows the enlarged 1510-1590 cm⁻¹ region associated with carboxylate group vibrations. (B) Degree of ionization of linear and star PAA within 30-bilayer PAA/PDMAEMA films deposited at pH 2.5 calculated as $(A_{v_{COO^-}}/[A_{v_{COO^+}}+A_{v_{COOH}}])*100\%$, where A are the absorbances of the corresponding bands. (C) Schematic representation of multilayer assembly of LPAA/PDMAEMA (left) and 8PAA/PDMAEMA (right).

 (v_{COO}) and non-ionized (v_{COOH}) carboxylic groups of PAA are distinct (1560 cm⁻¹ and 1710 cm⁻¹ ¹, respectively) and can be used to estimate the ionization of polyacids within LbL films, assuming that the extinction coefficients of these bands are equal. ³⁰ Fig. 4A shows that the peak at 1560 cm⁻ ¹ associated with stretching vibrations of the ionized carboxylic groups decreased with the number of arms in PAA, indicating lower ionization of star polymers within LbL films. To quantify these changes, the carbonyl region of the spectra was deconvoluted to account for the contribution of stretching vibrations of the ester groups of PDMAEMA, $v_{C=0}$ at ~1735 cm⁻¹ (the deconvolution procedure is described in the experimental section), and ionization of assembled PAAs was calculated as the ratio of v_{COO} absorbances to the sum of v_{COO} and v_{COOH} absorbances. Fig. 4B shows that ionization of PAA decreased ~2-fold with the increase in polymer branching, indicating a reduction in the number of ionic pairs within star PAA/PDMAEMA relative to LPAA/PDMAEMA films as illustrated in Fig. 4C. Note that the ionization degree of LPAA reported here (~14 %) falls between values previously found with LbL films of PAA, ~25% for PAA/PAH³⁰ and ~4% for PAA/PDADMAC³¹ films deposited at the same pH 2.5. This result reflects the competing effects of the strength of ionic pairing and steric hindrance at the amino group of a polycationic partner on the ionization of the assembled polyacids. Consistent with these findings is the linear deposition character of PAA/PAH films 60 versus exponential growth in PAA/PDMAMAC,³¹ which further illustrates the important role of the polycationic partner on the intermolecular binding and growth modes of multilayers of weak polyelectrolytes.⁴⁹

Deposition of LbL films can be correlated with the formation of interpolymer complexes (IPC) in solution.⁶¹⁻⁶³ Thus, differences in ionic paring within *L*PAA/PDMAEMA and star PAA/PDMAEMA systems were further explored using ITC. This technique was previously used to study correlations between the enthalpy of intermolecular binding and the growth mode of

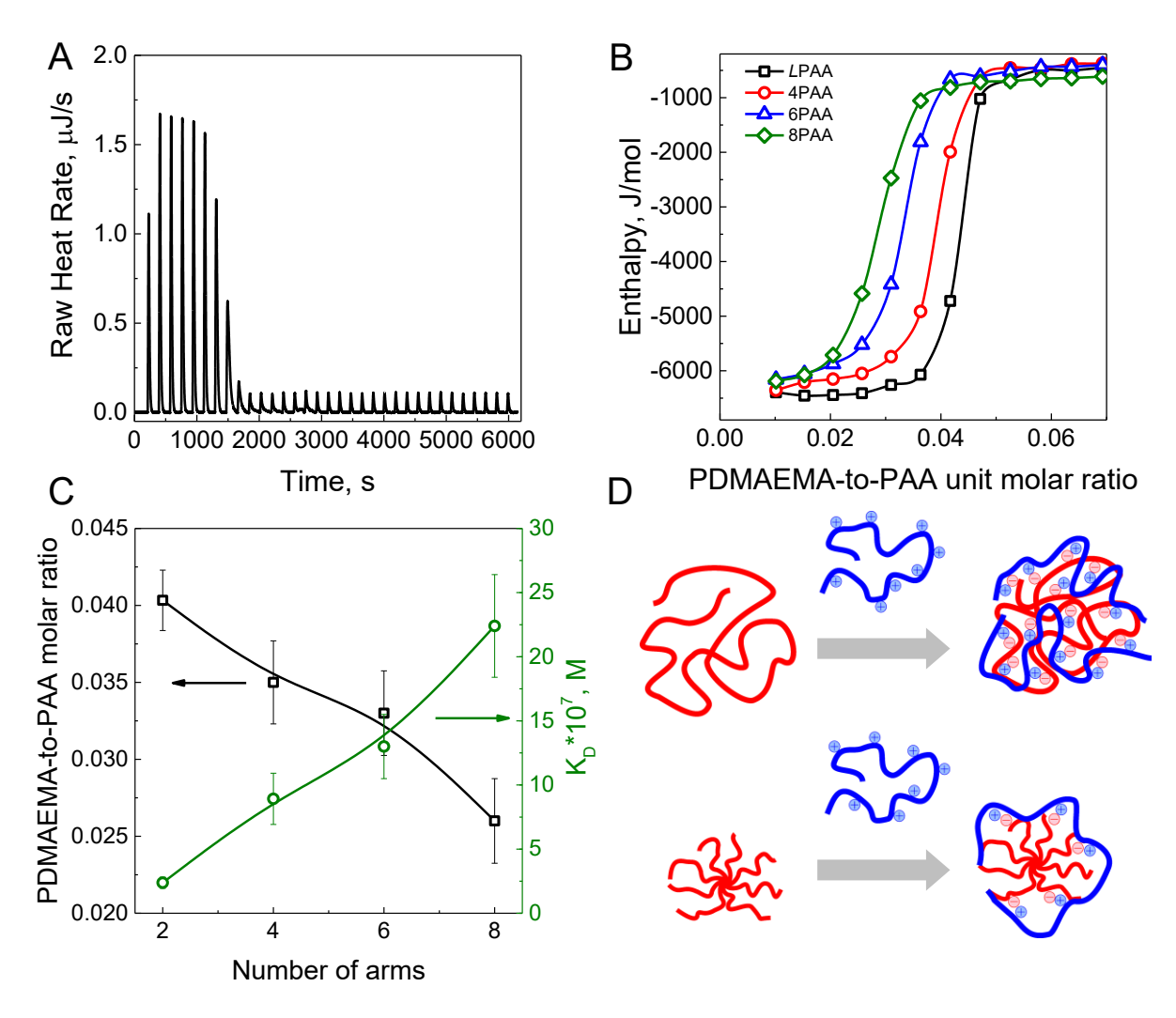


Fig. 5. (A) Representative ITC titration curve of a 0.5 mg/ml *L*PAA (7 mM of polymer units) solution with a 0.63 mg/ml PDMAEMA (4 mM of polymer units) solution at pH 2.5. (B) A plot of enthalpy vs PDMAEMA-to-PAA unit molar ratio for *L*PAA/PDMAEMA (squares), 4PAA/PDMAEMA (circles), 6PAA/PDMAEMA (triangles), 8PAA/PDMAEMA (diamonds) systems. (C) The impact of polymer branching on PDMAEMA-to-PAA ratio of units (squares) and dissociation constant (K_D) (circles). All titrations were performed at 25 °C. The error bars show the 95% confidence intervals determined from three repeated independent measurements. (D) Schematic representation of interpolymer complexes of *L*PAA or 8PAA with PDMAEMA at pH 2.5.

electrostatic LbL films, as well as the role of a hydrogen-bonding competitor, polymer branching and a binding partner on interpolymer hydrogen-bonding.⁶³⁻⁶⁷ **Figs. 5A** and **S12** show raw ITC

data for the titration of linear and star PAAs, respectively, with PDMAEMA at pH 2.5. Interestingly, in all cases, the enthalpies of polymer-polymer interactions (ΔH_{int}) after saturation of PAA with PDMAEMA were similar (~ -5.5 kJ per mole of PDMAEMA units) (Fig. 5B). Previous studies correlated ΔH_{int} with the growth regime of electrostatic LbL films, suggesting that the exponential growth mode is observed for polymer pairs whose formation is endothermic.⁶³ In this work, however, we observed that the exponentially grown PAA/PDMAEMA film has negative ΔH_{int} suggesting strong entropic contributions, such as those associated with release of water molecules and counterions, on the film growth mode. Interestingly, the limiting composition of PAA/PDMAEMA IPCs achieved after saturation of PAA with PDMAEMA was dependent on the degree of PAA branching, with more branched PAAs containing less PDMAEMA (Fig. 5B, C). This result can be rationalized as more compact star PAA forming ionic pairs with PDMAEMA and likely preferentially interacting with the peripheral units of the star polymers. Note that this result is different from what was observed in hydrogen-bonded complexes of linear poly(methacrylic acid) (PMAA) with star poly(ethylene oxide) (PEO), where star PEO provided a higher density of hydrogen-bonded sites leading to higher enthalpy and higher content of PMAA within its complexes with star PEO. 65 In the system described here and in the selected conditions of our experiments of pH 2.5, IPCs were stabilized by electrostatic rather than hydrogen bonding interactions, while protonation of PAA units competed with PDMAEMA-induced ionization, and possibly supported dimerization of carboxylic groups in the higher density environment of the star polymers. In agreement with a smaller number of ionic contacts being formed by star PAAs with PDMAEMA, the dissociation constant (K_D) calculated from the ITC results was up to one order of magnitude higher for star PAAs. The weaker binding of star PAAs with PDMAEMA in solution correlates with enhanced diffusion of star polymers within LbL films and demonstrates the

insufficiency of only invoking star polymer compactness to explain the greater mobility in LbL assemblies. We believe that in addition to star polymer compactness, a lower number of ionic contacts formed by star PAAs within LbL films contributes collectively to the significantly higher mobility of star PAAs observed in this work.

In summary, we have explored the effect of molecular architecture on diffusion and quantitively determined the diffusion coefficients for both star polyacid and polycation within LbL films. Our findings of faster diffusion of star polyacids are qualitatively similar to previous reports of faster diffusion for star polymers in solution in comparison to their linear counterparts, ^{53, 68} as well as higher mobility of star polymers within LbL films. ²¹ However, here we quantitatively explore the origins of such enhanced mobility and show that in addition to the standard argument of polymer compactness, the number of contacts with linear partners plays an even more important role in determining the dynamics of assembled polymers of different molecular architecture. We have established experimental pathways for quantifying the number of binding sites for assembled weak polyacids using FTIR and ITC techniques and correlated these results with molecular diffusion coefficients obtained by NR and *in situ* ellipsometry. The fundamental insights on the behavior of assembled star polymers established in this work can serve as a framework for rational engineering of ultrathin films for applications such as controlled drug delivery.

Acknowledgments:

This work was supported by the National Science Foundation under Award DMR-1905535 (S.S). The use of the TAMU Soft Matter Facility is acknowledged. Neutron measurements were performed at the Spallation Neutron Source at the Oak Ridge National Laboratory, managed by UT-Battelle, LLC, for the DOE under contract No. DE-AC05-000R22725.

Supporting information: NMR data of star polymer initiators, linear and star polymer characterization using GPC, potentiometric titration of linear and star PAA, AFM images of prime layer and PAA/PDMAEMA films, schematic representation and fitting parameters of neutron reflectivity studies, raw ITC data of titration of star PAAs with PDMAEMA.

References:

- 1. Ren, J. M.; McKenzie, T. G.; Fu, Q.; Wong, E. H. H.; Xu, J.; An, Z.; Shanmugam, S.; Davis, T. P.; Boyer, C.; Qiao, G. G., Star Polymers. *Chemical Reviews* **2016**, *116* (12), 6743-6836.
- 2. Cosimbescu, L.; Robinson, J. W.; Zhou, Y.; Qu, J., Dual functional star polymers for lubricants. *RSC Advances* **2016**, *6* (89), 86259-86268.
- 3. van Ravensteijn, B. G. P.; Bou Zerdan, R.; Seo, D.; Cadirov, N.; Watanabe, T.; Gerbec, J. A.; Hawker, C. J.; Israelachvili, J. N.; Helgeson, M. E., Triple Function Lubricant Additives Based on Organic–Inorganic Hybrid Star Polymers: Friction Reduction, Wear Protection, and Viscosity Modification. *ACS Applied Materials & Interfaces* **2019**, *11* (1), 1363-1375.
- 4. Giuntoli, A.; Hansoge, N. K.; Keten, S., Star topology increases ballistic resistance in thin polymer films. *Extreme Mechanics Letters* **2020**, *41*, 101038.
- 5. Giuntoli, A.; Keten, S., Tuning star architecture to control mechanical properties and impact resistance of polymer thin films. *Cell Reports Physical Science* **2021**, *2* (10), 100596.
- 6. Lotocki, V.; Kakkar, A., Miktoarm Star Polymers: Branched Architectures in Drug Delivery. *Pharmaceutics* **2020**, *12* (9), 827.
- 7. Wu, W.; Wang, W.; Li, J., Star polymers: Advances in biomedical applications. *Progress in Polymer Science* **2015**, *46*, 55-85.
- 8. Wiltshire, J. T.; Qiao, G. G., Recent Advances in Star Polymer Design: Degradability and the Potential for Drug Delivery. *Australian Journal of Chemistry* **2007**, *60* (10), 699-705.
- 9. Georgiou, T. K., Star polymers for gene delivery. *Polymer International* **2014**, *63* (7), 1130-1133.

- 10. Gao, H., Development of Star Polymers as Unimolecular Containers for Nanomaterials. *Macromolecular Rapid Communications* **2012**, *33* (9), 722-734.
- 11. Taghavi-Kahagh, A.; Safavi-Mirmahalleh, S.-A.; Pashaei-Sarnaghi, R.; Salami-Kalajahi, M.; Roghani-Mamaqani, H., Polyampholyte poly[2-(dimethylamino)ethyl methacrylate]-starpoly(methacrylic acid) star copolymers as colloidal drug carriers. *Journal of Molecular Liquids* **2021**, *335*, 116247.
- 12. Aliakseyeu, A.; Hlushko, R.; Sukhishvili, S. A., Nonionic star polymers with upper critical solution temperature in aqueous solutions. *Polymer Chemistry* **2022**, *13* (18), 2637-2650.
- 13. Huang, H.; Tang, G.; Wang, Q.; Li, D.; Shen, F.; Zhou, J.; Yu, H., Two novel non-viral gene delivery vectors: low molecular weight polyethylenimine cross-linked by (2-hydroxypropyl)-β-cyclodextrin or (2-hydroxypropyl)-γ-cyclodextrin. *Chemical Communications* **2006**, (22), 2382-2384.
- 14. Yang, C.; Li, H.; Goh, S. H.; Li, J., Cationic star polymers consisting of α-cyclodextrin core and oligoethylenimine arms as nonviral gene delivery vectors. *Biomaterials* **2007**, *28* (21), 3245-3254.
- 15. Chen, X.; Wu, W.; Guo, Z.; Xin, J.; Li, J., Controlled insulin release from glucosesensitive self-assembled multilayer films based on 21-arm star polymer. *Biomaterials* **2011**, *32* (6), 1759-1766.
- 16. Zhou, Q.; Palanisamy, A.; Albright, V.; Sukhishvili, S. A., Enzymatically degradable star polypeptides with tunable UCST transitions in solution and within layer-by-layer films. *Polymer Chemistry* **2018**, *9* (40), 4979-4983.

- 17. Albright, V.; Palanisamy, A.; Zhou, Q.; Selin, V.; Sukhishvili, S. A., Functional Surfaces through Controlled Assemblies of Upper Critical Solution Temperature Block and Star Copolymers. *Langmuir* **2019**, *35* (33), 10677-10688.
- 18. Connal, L. A.; Li, Q.; Quinn, J. F.; Tjipto, E.; Caruso, F.; Qiao, G. G., pH-Responsive Poly(acrylic acid) Core Cross-Linked Star Polymers: Morphology Transitions in Solution and Multilayer Thin Films. *Macromolecules* **2008**, *41* (7), 2620-2626.
- 19. Kim, B.-S.; Gao, H.; Argun, A. A.; Matyjaszewski, K.; Hammond, P. T., All-Star Polymer Multilayers as pH-Responsive Nanofilms. *Macromolecules* **2009**, *42* (1), 368-375.
- 20. Guo, Z.; Chen, X.; Xin, J.; Wu, D.; Li, J.; Xu, C., Effect of Molecular Weight and Arm Number on the Growth and pH-Dependent Morphology of Star Poly[2-(dimethylamino)ethyl methacrylate]/Poly(styrenesulfonate) Multilayer Films. *Macromolecules* **2010**, *43* (21), 9087-9093.
- 21. Choi, I.; Suntivich, R.; Plamper, F. A.; Synatschke, C. V.; Müller, A. H. E.; Tsukruk, V. V., pH-Controlled Exponential and Linear Growing Modes of Layer-by-Layer Assemblies of Star Polyelectrolytes. *Journal of the American Chemical Society* **2011**, *133* (24), 9592-9606.
- 22. Chen, F.; Liu, G.; Zhang, G., Formation of Multilayers by Star Polyelectrolytes: Effect of Number of Arms on Chain Interpenetration. *The Journal of Physical Chemistry B* **2012**, *116* (35), 10941-10950.
- 23. Liu, W.; Wijeratne, S.; Yang, L.; Bruening, M., Porous star-star polyelectrolyte multilayers for protein binding. *Polymer* **2018**, *138*, 267-274.
- 24. Mendrek, B.; Trzebicka, B., Synthesis and characterization of well-defined poly(tert-butyl acrylate) star polymers. *European Polymer Journal* **2009**, *45* (7), 1979-1993.

- 25. Xu, L.; Kozlovskaya, V.; Kharlampieva, E.; Ankner, J. F.; Sukhishvili, S. A., Anisotropic Diffusion of Polyelectrolyte Chains within Multilayer Films. *ACS Macro Letters* **2012**, *1* (1), 127-130.
- 26. Selin, V.; Ankner, J. F.; Sukhishvili, S. A., Nonlinear Layer-by-Layer Films: Effects of Chain Diffusivity on Film Structure and Swelling. *Macromolecules* **2017**, *50* (16), 6192-6201.
- 27. Sukhishvili, S. A.; Granick, S., Layered, Erasable Polymer Multilayers Formed by Hydrogen-Bonded Sequential Self-Assembly. *Macromolecules* **2002**, *35* (1), 301-310.
- 28. Kharlampieva, E.; Sukhishvili, S. A., Polyelectrolyte Multilayers of Weak Polyacid and Cationic Copolymer: Competition of Hydrogen-Bonding and Electrostatic Interactions. *Macromolecules* **2003**, *36* (26), 9950-9956.
- 29. Kharlampieva, E.; Sukhishvili, S. A., Ionization and pH Stability of Multilayers Formed by Self-Assembly of Weak Polyelectrolytes. *Langmuir* **2003**, *19* (4), 1235-1243.
- 30. Choi, J.; Rubner, M. F., Influence of the Degree of Ionization on Weak Polyelectrolyte Multilayer Assembly. *Macromolecules* **2005**, *38* (1), 116-124.
- 31. Bütergerds, D.; Kateloe, C.; Cramer, C.; Schönhoff, M., Influence of the degree of ionization on the growth mechanism of poly(diallyldimethylammonium)/poly(acrylic acid) multilayers. *Journal of Polymer Science Part B: Polymer Physics* **2017**, *55* (5), 425-434.
- 32. Nestler, P.; Paßvogel, M.; Helm, C. A., Influence of Polymer Molecular Weight on the Parabolic and Linear Growth Regime of PDADMAC/PSS Multilayers. *Macromolecules* **2013**, *46* (14), 5622-5629.
- 33. Ghostine, R. A.; Markarian, M. Z.; Schlenoff, J. B., Asymmetric Growth in Polyelectrolyte Multilayers. *Journal of the American Chemical Society* **2013**, *135* (20), 7636-7646.

- 34. Vikulina, A. S.; Anissimov, Y. G.; Singh, P.; Prokopović, V. Z.; Uhlig, K.; Jaeger, M.
- S.; von Klitzing, R.; Duschl, C.; Volodkin, D., Temperature effect on the build-up of exponentially growing polyelectrolyte multilayers. An exponential-to-linear transition point. *Physical Chemistry Chemical Physics* **2016**, *18* (11), 7866-7874.
- 35. Picart, C.; Mutterer, J.; Richert, L.; Luo, Y.; Prestwich, G. D.; Schaaf, P.; Voegel, J. C.; Lavalle, P., Molecular basis for the explanation of the exponential growth of polyelectrolyte multilayers. *Proceedings of the National Academy of Sciences* **2002**, *99* (20), 12531.
- 36. Lavalle, P.; Gergely, C.; Cuisinier, F. J. G.; Decher, G.; Schaaf, P.; Voegel, J. C.; Picart, C., Comparison of the Structure of Polyelectrolyte Multilayer Films Exhibiting a Linear and an Exponential Growth Regime: An in Situ Atomic Force Microscopy Study. *Macromolecules* **2002**, *35* (11), 4458-4465.
- 37. Palumbo, M.; Pearson, C.; Petty, M. C., Atomic force microscope characterization of poly(ethyleneimine)/poly(ethylene-co-maleic acid) and poly(ethyleneimine)/poly(styrene sulfonate) multilayers. *Thin Solid Films* **2005**, *483* (1), 114-121.
- 38. Podsiadlo, P.; Shim, B. S.; Kotov, N. A., Polymer/clay and polymer/carbon nanotube hybrid organic—inorganic multilayered composites made by sequential layering of nanometer scale films. *Coordination Chemistry Reviews* **2009**, *253* (23), 2835-2851.
- 39. Dubas, S. T.; Schlenoff, J. B., Swelling and Smoothing of Polyelectrolyte Multilayers by Salt. *Langmuir* **2001**, *17* (25), 7725-7727.
- 40. McAloney, R. A.; Dudnik, V.; Goh, M. C., Kinetics of Salt-Induced Annealing of a Polyelectrolyte Multilayer Film Morphology. *Langmuir* **2003**, *19* (9), 3947-3952.
- 41. Chremos, A.; Camp, P. J.; Glynos, E.; Koutsos, V., Adsorption of star polymers: computer simulations. *Soft Matter* **2010**, *6* (7), 1483-1493.

- 42. Soltwedel, O.; Ivanova, O.; Nestler, P.; Müller, M.; Köhler, R.; Helm, C. A., Interdiffusion in Polyelectrolyte Multilayers. *Macromolecules* **2010**, *43* (17), 7288-7293.
- 43. Sill, A.; Nestler, P.; Thran, P.; Helm, C. A., Dependence of PSS Diffusion in Multilayers of Entangled PDADMA on Temperature and Salt Concentration: More than One Diffusion Constant. *Macromolecules* **2021**, *54* (20), 9372-9384.
- 44. Selin, V.; Ankner, J. F.; Sukhishvili, S. A., Diffusional Response of Layer-by-Layer Assembled Polyelectrolyte Chains to Salt Annealing. *Macromolecules* **2015**, *48* (12), 3983-3990.
- 45. Aliakseyeu, A.; Albright, V.; Yarbrough, D.; Hernandez, S.; Zhou, Q.; Ankner, J. F.; Sukhishvili, S. A., Selective hydrogen bonding controls temperature response of layer-by-layer upper critical solution temperature micellar assemblies. *Soft Matter* **2021**, *17* (8), 2181-2190.
- 46. Kozlovskaya, V.; Stockmal, K. A.; Higgins, W.; Ankner, J. F.; Morgan, S. E.; Kharlampieva, E., Architecture of Hydrated Multilayer Poly(methacrylic acid) Hydrogels: The Effect of Solution pH. *ACS Applied Polymer Materials* **2020**, *2* (6), 2260-2273.
- 47. Hlushko, R.; Ankner, J. F.; Sukhishvili, S., Dynamics and Self-Healing of Layer-by-Layer Hydrogen-Bonded Films of Linear Synthetic Polyphenols. *Macromolecules* **2021**, *54* (16), 7469-7479.
- 48. Jomaa, H. W.; Schlenoff, J. B., Salt-Induced Polyelectrolyte Interdiffusion in Multilayered Films: A Neutron Reflectivity Study. *Macromolecules* **2005**, *38* (20), 8473-8480.
- 49. Xu, L.; Ankner, J. F.; Sukhishvili, S. A., Steric Effects in Ionic Pairing and Polyelectrolyte Interdiffusion within Multilayered Films: A Neutron Reflectometry Study. *Macromolecules* **2011**, *44* (16), 6518-6524.
- 50. Zan, X.; Peng, B.; Hoagland, D. A.; Su, Z., Polyelectrolyte uptake by PEMs: Impact of salt concentration. *Polymer Chemistry* **2011**, *2* (11), 2581-2589.

- 51. Fares, H. M.; Schlenoff, J. B., Diffusion of Sites versus Polymers in Polyelectrolyte Complexes and Multilayers. *Journal of the American Chemical Society* **2017**, *139* (41), 14656-14667.
- 52. Comyn, J., Introduction to Polymer Permeability and the Mathematics of Diffusion. In *Polymer Permeability*, Comyn, J., Ed. Springer Netherlands: Dordrecht, 1985; pp 1-10.
- 53. Xuexin, C.; Zhongde, X.; Von Meerwall, E.; Seung, N.; Hadjichristidis, N.; Fetters, L. J., Self-diffusion of linear and 4- and 18-armed star polyisoprenes in tetrachloromethane solution. *Macromolecules* **1984**, *17* (7), 1343-1348.
- 54. Robello, D. R.; André, A.; McCovick, T. A.; Kraus, A.; Mourey, T. H., Synthesis and Characterization of Star Polymers Made from Simple, Multifunctional Initiators. *Macromolecules* **2002**, *35* (25), 9334-9344.
- 55. Lue, L.; Kiselev, S. B., Star Polymers in Good Solvents from Dilute to Concentrated Regimes: Crossover Approach. *Condensed Matter Physics* **2002**, *5*, 73-104.
- 56. Plet, L.; Delecourt, G.; Hanafi, M.; Pantoustier, N.; Pembouong, G.; Midoux, P.; Bennevault, V.; Guégan, P., Controlled star poly(2-oxazoline)s: Synthesis, characterization. *European Polymer Journal* **2020**, *122*, 109323.
- 57. Chremos, A.; Jeong, C.; Douglas, J. F., Influence of polymer architectures on diffusion in unentangled polymer melts. *Soft Matter* **2017**, *13* (34), 5778-5784.
- 58. Huber, K.; Burchard, W.; Fetters, L. J., Dynamic light scattering from regular star-branched molecules. *Macromolecules* **1984**, *17* (4), 541-548.
- 59. Plamper, F. A.; Becker, H.; Lanzendörfer, M.; Patel, M.; Wittemann, A.; Ballauff, M.; Müller, A. H. E., Synthesis, Characterization and Behavior in Aqueous Solution of Star-Shaped Poly(acrylic acid). *Macromolecular Chemistry and Physics* **2005**, *206* (18), 1813-1825.

- 60. Yoo, D.; Shiratori, S. S.; Rubner, M. F., Controlling Bilayer Composition and Surface Wettability of Sequentially Adsorbed Multilayers of Weak Polyelectrolytes. *Macromolecules* **1998**, *31* (13), 4309-4318.
- 61. Sukhishvili, S. A.; Kharlampieva, E.; Izumrudov, V., Where Polyelectrolyte Multilayers and Polyelectrolyte Complexes Meet. *Macromolecules* **2006**, *39* (26), 8873-8881.
- 62. Xu, L.; Pristinski, D.; Zhuk, A.; Stoddart, C.; Ankner, J. F.; Sukhishvili, S. A., Linear versus Exponential Growth of Weak Polyelectrolyte Multilayers: Correlation with Polyelectrolyte Complexes. *Macromolecules* **2012**, *45* (9), 3892-3901.
- 63. Laugel, N.; Betscha, C.; Winterhalter, M.; Voegel, J.-C.; Schaaf, P.; Ball, V., Relationship between the Growth Regime of Polyelectrolyte Multilayers and the Polyanion/Polycation Complexation Enthalpy. *The Journal of Physical Chemistry B* **2006**, *110* (39), 19443-19449.
- 64. Selin, V.; Aliakseyeu, A.; Ankner, J. F.; Sukhishvili, S. A., Effect of a Competitive Solvent on Binding Enthalpy and Chain Intermixing in Hydrogen-Bonded Layer-by-Layer Films. *Macromolecules* **2019**, *52* (12), 4432-4440.
- 65. Aliakseyeu, A.; Dormidontova, E. E.; Sukhishvili, S. A., Hydrogen-Bonded Complexes of Star Polymers. *Macromolecular Rapid Communications* **2021,** *42* (12), 2100097.
- 66. Bizley, S. C.; Williams, A. C.; Khutoryanskiy, V. V., Thermodynamic and kinetic properties of interpolymer complexes assessed by isothermal titration calorimetry and surface plasmon resonance. *Soft Matter* **2014**, *10* (41), 8254-8260.
- 67. Alonso, T.; Irigoyen, J.; Iturri, J. J.; larena, I. L.; Moya, S. E., Study of the multilayer assembly and complex formation of poly(diallyldimethylammonium chloride) (PDADMAC) and poly(acrylic acid) (PAA) as a function of pH. *Soft Matter* **2013**, *9* (6), 1920-1928.

68. Von Meerwall, E.; Tomich, D. H.; Grigsby, J.; Pennisi, R. W.; Fetters, L. J.; Hadjichristidis, N., Self-diffusion of three-armed star and linear polybutadienes and polystyrenes in tetrachloromethane solution. *Macromolecules* **1983**, *16* (11), 1715-1722.